

Lazertinib improves the efficacy of chemotherapeutic drugs in ABCB1 or ABCG2 overexpression cancer cells *in vitro*, *in vivo*, and *ex vivo*

Yingfang Fan,^{1,4} Tian Tao,^{1,2,4} Zhixing Guo,² Kenneth Kin Wah To,³ Da Chen,² Shaorong Wu,² Chuan Yang,² Jinsui Li,¹ Min Luo,² Fang Wang,² and Liwu Fu²

¹Zhujiang Hospital, Southern Medical University, The Second School of Clinical Medicine, Southern Medical University, Guangzhou 510260, China; ²Collaborative Innovation Center for Cancer Medicine, State Key Laboratory of Oncology in South China, Guangdong Esophageal Cancer Institute, Guangzhou, Sun Yat-Sen University Cancer Center, Guangzhou 510060, China; ³School of Pharmacy, The Chinese University of Hong Kong, Hong Kong, China

Multidrug resistance (MDR) is the major cause of chemotherapy failure, which is usually caused by the overexpression of ATP-binding cassette (ABC) transporters such as ABCB1 and ABCG2. To date, no MDR modulator has been clinically approved. Here, we found that lazertinib (YH25448; a novel third-generation tyrosine kinase inhibitor [TKI]) could enhance the anticancer efficacy of MDR transporter substrate anticancer drugs *in vitro*, *in vivo*, and *ex vivo*. Mechanistically, lazertinib was shown to inhibit the drug efflux activities of ABCB1 and ABCG2 and thus increase the intracellular accumulation of the transporter substrate anticancer drug. Moreover, lazertinib was found to stimulate the ATPase activity of ABCB1/ABCG2 and inhibit the photolabeling of the transporters by ¹²⁵I-iodoarylazidoprazosin (IAAP). However, lazertinib neither changed the expression or localization of ABCB1 and ABCG2 nor blocked the signal pathway of Akt or Erk1/2 at a drug concentration effective for MDR reversal. Overall, our results demonstrate that lazertinib effectively reverses ABCB1- or ABCG2-mediated MDR by competitively binding to the ATP-binding site and inhibiting drug efflux function. This is the first report demonstrating the novel combined use of lazertinib and conventional chemotherapeutic drugs to overcome MDR in ABCB1/ABCG2-overexpressing cancer cells.

INTRODUCTION

Drug resistance is a major obstacle to cancer chemotherapy. Multidrug resistance (MDR) refers to the phenomenon where cancer cells become unresponsive simultaneously to various structurally and mechanistically different chemotherapeutic agents during or after a short period of treatment.^{1,2} Numerous mechanisms are known to cause MDR, which include overexpression of ATP-binding cassette (ABC) drug efflux transporters, elevated metabolism of xenobiotic drugs, abnormal apoptosis regulation, increased DNA repair, and tumor microenvironment (TME).^{3,4} It is noteworthy that overexpression of the ABC transporter family is the most common mechanism driving chemoresistance by increasing the efflux of various anticancer drugs.^{5–7} ABC transporter proteins consist of nucleotide-binding do-

main (NBDs) and transmembrane domains (TMDs). Upon binding of substrates to TMDs of ABC transporters, conformation of the transporter protein is changed, and the NBDs bind with ATP to trigger its hydrolysis to release energy to mediate efflux of the substrate drug.⁸ Recently, our research team has demonstrated the intercellular transfer of an extensively studied ABC transporter (P-gp/ABCB1) via exosome to induce the spread of MDR.^{9,10}

In humans, 49 ABC transporters have been identified, and they are classified into seven subfamilies (ABCA–ABCG) according to their amino acid sequence.^{11,12} Among all ABC transporters, ABCB1, ABCC1, and ABCG2 have been extensively studied, and they are associated with MDR in cancer cells.^{13,14} ABCB1, also commonly known as P-glycoprotein (P-gp), is highly expressed in many vital organs, including liver, kidney, lung, placenta, and intestine, for protection and detoxification.¹⁵ ABCB1 is known to mediate MDR to numerous anticancer drugs such as vincristine, paclitaxel, doxorubicin, colchicine, vinblastine, and etoposide by pumping them out of drug-resistant cancer cells.^{16,17} ABCG2, also known as breast cancer resistance protein (BCRP), is highly expressed in many tissues, including the mammary glands, prostate, small intestine, brain, colon, liver, and kidney.^{18,19} It acts as an essential component of the cell defense system and is also associated with cell stemness.^{15,20} ABCG2 is known to mediate MDR to numerous anticancer drugs including topotecan, mitoxantrone, irinotecan, and SN-38.

To overcome the drug resistance mediated by ABC transporters, four generations of ABC transporter modulators have been reported. However, the clinical applications of these modulators are mostly limited

Received 9 June 2021; accepted 3 February 2022;
<https://doi.org/10.1016/j.omto.2022.02.006>.

⁴These authors contributed equally

Correspondence: Liwu Fu, Collaborative Innovation Center for Cancer Medicine, State Key Laboratory of Oncology in South China, Guangdong Esophageal Cancer Institute, Guangzhou, Sun Yat-Sen University Cancer Center, Guangzhou 510060, China

E-mail: fulw@mail.sysu.edu.cn



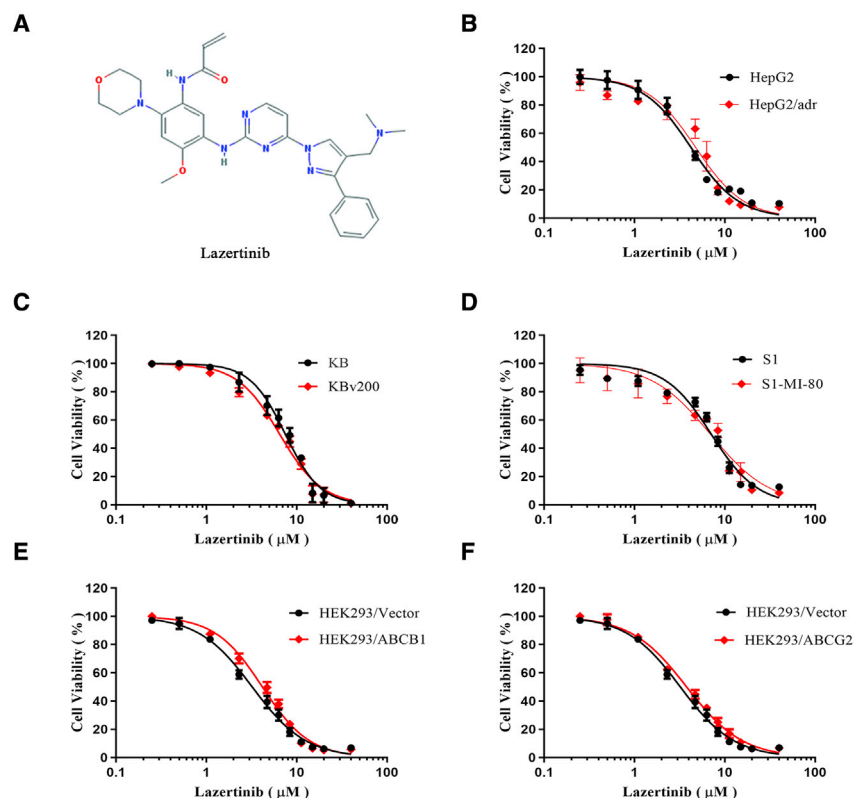


Figure 1. Structure and cytotoxicity of lazertinib

(A) The structural formula of lazertinib. Cytotoxicity of lazertinib alone was evaluated using the MTT assay in (B) HepG2 and HepG2/adr cells, (C) KB and KBv200 cells, (D) S1 and S1-MI-80 cells, (E) HEK293/Vector and HEK293/ABCB1 cells, (F) HEK293/Vector and HEK293/ABCG2 cells. The cells were incubated with a range of different concentrations of lazertinib for 72 h. Means \pm SD values from three independent experiments are presented.

due to significant toxicity, lack of specificity, and undesirable drug-drug interactions.^{21–23} Therefore, there is an unmet medical need for novel and potent MDR modulators suitable for clinical use in cancer patients.

Tyrosine kinase inhibitors (TKIs) are small molecular compounds widely used in the clinic for targeted cancer therapy via interfering the binding of ATP at the tyrosine kinase domain of important oncogenic signaling molecules.²⁴ Interestingly, some TKIs were also found to bind to the ATP-binding site of ABC transporters, thus inhibiting their drug transport function. Our research team has previously reported the inhibition of ABC transporters and reversal of MDR by numerous TKIs, including rociletinib,²⁵ alectinib,²⁶ afatinib,²⁷ osimertinib,²⁸ lapatinib,²⁹ erk5-in-1,³⁰ and CM082.³¹ Lazertinib (YH25448) is a novel third-generation, irreversible, and wild-type-sparing EGFR TKI recently approved for advanced non-small-cell lung cancer patients progressing after first- and second-generation EGFR TKI therapy and harboring a defined tumor T790M status.^{32,33} In the present study, the possible reversal of ABC transporter-mediated MDR by lazertinib was investigated.

RESULTS

Lazertinib significantly reversed MDR in cancer cells overexpressing ABCB1 or ABCG2 *in vitro*

The cytotoxicity of lazertinib alone was first determined by the MTT assay. As indicated, 0.25 μ M lazertinib was chosen as the highest concentration used in the MDR reversal studies because approximately

90% of cells (both drug-sensitive and drug-resistant cells) remain viable after lazertinib treatment at this concentration (Figures 1B–1F). As shown in Table 1 and Table 2, compared with the drug sensitive cells the ABCB1-overexpressing MDR cells (KBv200, HepG2/adr, and HEK293/ABCB1) and ABCG2-overexpressing MDR cells (S1-MI-80 and HEK293/ABCG2) are remarkably resistant to substrate drugs. However, and importantly, in the presence of lazertinib, lower IC₅₀ values of the transporter substrate anticancer agents were achieved in the drug-resistant cells. However, lazertinib did not appreciably change the IC₅₀ values of the same anticancer drugs in the sensitive parental cells, or the IC₅₀ values for the non-substrate drug (i.e., cisplatin) in both drug-resistant and drug-sensitive cells. Collectively, our results suggested that lazertinib specifically potentiated the efficacy of MDR transporter substrate chemotherapeutic drugs in ABCB1- or ABCG2-overexpressing cancer cells.

Lazertinib reversed ABCB1-mediated MDR *in vivo*

In order to evaluate the MDR reversal effect of lazertinib *in vivo*, the ABCB1-overexpressing HepG2/adr xenograft model in nude mouse was used. A photograph of the harvested tumor xenograft at the end of the 28-day observation period is shown in Figure 2A. The tumor xenograft was not responsive to doxorubicin (DOX) alone (2 mg/kg) or lazertinib alone (10 mg/kg), because the tumor size was not appreciably different from that of the saline group (Figure 2B). However, a remarkable decrease in tumor size (Figure 2B) and tumor weight (Figure 2C) was observed in the combination of lazertinib and DOX compared with the saline group or the DOX-alone group. Moreover, no obvious change in mouse body weight was observed in all treatment groups (Figure 2D), suggesting that the combination therapy was generally well tolerated. Taken together, the results indicated that lazertinib effectively reversed ABCB1-mediated MDR at non-toxic doses *in vivo*.

Lazertinib enhanced the efficacy of the substrate drug in ABCB1-overexpressing human tumor specimens

In order to explore the clinical relevance of combination therapy of lazertinib and traditional chemotherapeutic drugs, clinical specimens of hepatocellular carcinoma were used in *ex vivo* experiment. The

Table 1. Effect of lazertinib on reversing the MDR mediated by ABCB1 or ABCG2 in drug selected resistant cancer cells

Compounds	IC ₅₀ ± SD (μM) (fold reversal)			
	KB (parental)		KBv200 (ABCB1)	
Vincristine	0.0059 ± 0.0323	(1.00)	0.2263 ± 0.0323	(1.00)
+0.0625 μM Lazertinib	0.0053 ± 0.0003	(1.12)	0.0782 ± 0.0182**	(2.89)
+0.125 μM Lazertinib	0.0041 ± 0.0002	(1.43)	0.0195 ± 0.0105**	(11.60)
+0.25 μM Lazertinib	0.0050 ± 0.0007	(1.54)	0.0090 ± 0.0011**	(25.21)
+10 μM Verapamil	0.0042 ± 0.0002	(1.47)	0.0100 ± 0.0038**	(22.60)
Doxorubicin	0.0218 ± 0.0038	(1.00)	1.2091 ± 0.4592	(1.00)
+0.0625 μM Lazertinib	0.0216 ± 0.0093	(1.01)	0.4347 ± 0.0807**	(2.76)
+0.125 μM Lazertinib	0.0190 ± 0.0038	(1.13)	0.2066 ± 0.0872**	(5.85)
+0.25 μM Lazertinib	0.0203 ± 0.0030	(1.07)	0.1535 ± 0.0698**	(7.87)
+10 μM Verapamil	0.0209 ± 0.0140	(1.03)	0.1457 ± 0.0192**	(8.29)
Paclitaxel	0.0039 ± 0.00375	(1.00)	0.3045 ± 0.0145	(1.00)
+0.0625 μM Lazertinib	0.0021 ± 0.0005	(1.90)	0.0640 ± 0.0341**	(4.75)
+0.125 μM Lazertinib	0.0044 ± 0.0043	(0.89)	0.0474 ± 0.0425 **	(6.41)
+0.25 μM Lazertinib	0.0037 ± 0.0036	(1.06)	0.0191 ± 0.0178 **	(15.90)
+10 μM Verapamil	0.0361 ± 0.0034	(1.09)	0.0127 ± 0.0028 **	(23.97)
Cisplatin	0.6323 ± 0.0568	(1.00)	1.4709 ± 0.0416	(1.00)
+0.25 μM Lazertinib	1.2064 ± 0.1808	(0.5241)	1.7951 ± 0.0345	(0.82)
	HepG2 (parental)		HepG2/adr (ABCB1)	
Doxorubicin	0.5820 ± 0.1940	(1.00)	29.705 ± 12.535	(1.00)
+0.0625 μM Lazertinib	0.5556 ± 0.1852	(1.04)	5.5750 ± 0.0340**	(5.32)
+0.125 μM Lazertinib	0.4482 ± 0.1492	(1.29)	2.9670 ± 0.5621**	(10.01)
+0.25 μM Lazertinib	0.5571 ± 0.1857	(1.04)	2.0042 ± 0.0247**	(14.82)
+10 μM Verapamil	0.5191 ± 0.1730	(1.21)	0.4089 ± 0.0972**	(12.41)
Paclitaxel	0.0203 ± 0.0003	(1.00)	3.2675 ± 0.1025	(1.00)
+0.0625 μM Lazertinib	0.0174 ± 0.0021	(1.17)	2.4580 ± 0.0912	(1.32)
+0.125 μM Lazertinib	0.0084 ± 0.0021	(2.43)	1.0340 ± 0.0550**	(3.15)
+0.25 μM Lazertinib	0.0157 ± 0.00032	(1.29)	0.4071 ± 0.0241**	(8.02)
+10 μM Verapamil	0.0126 ± 0.0002	(1.61)	0.2638 ± 0.1260**	(12.38)
Cisplatin	1.1124 ± 0.0064	(1.00)	3.5702 ± 0.0500	(1.00)
+0.25 μM Lazertinib	1.0625 ± 0.0237	(1.04)	4.2824 ± 0.3864	(0.83)
	S1 (parental)		S1-MI-80 (ABCG2)	
Mitoxantrone	0.3123 ± 0.073	(1.00)	7.6202 ± 0.4067	(1.00)
+0.0625 μM Lazertinib	0.2423 ± 0.0061	(1.28)	5.7620 ± 0.3850	(1.33)
+0.125 μM Lazertinib	0.3209 ± 0.0262	(0.97)	2.4506 ± 0.1539**	(3.10)
+0.25 μM Lazertinib	0.2469 ± 0.0252	(1.26)	1.2175 ± 0.0367**	(6.25)
+2.5 μM FTC	0.2533 ± 0.0369	(1.23)	1.2791 ± 0.3631**	(5.95)
Topotecan	0.8309 ± 0.0400	(1.00)	6.0657 ± 0.1425	(1.00)
+0.0625 μM Lazertinib	0.7393 ± 0.0651	(1.12)	4.0421 ± 0.2348	(1.50)
+0.125 μM Lazertinib	0.7774 ± 0.0627	(1.06)	1.4407 ± 0.0574**	(4.21)
+0.25 μM Lazertinib	0.6006 ± 0.0026	(1.38)	0.9122 ± 0.0356**	(6.64)
+2.5 μM FTC	0.9061 ± 0.1203	(0.91)	0.6388 ± 0.4464**	(9.49)
Cisplatin	0.9972 ± 0.0036	(1.00)	3.1475 ± 0.0138	(1.00)
+0.25 μM Lazertinib	1.6369 ± 0.013	(0.61)	3.2288 ± 0.0262	(0.97)

The IC₅₀ of each drug was calculated by MTT assay, and the value represents means ± SD of three independent results. Setting the ratio of the IC₅₀ for chemotherapeutic agent alone versus the IC₅₀ for combination with lazertinib as the fold reversal of MDR. VRP and FTC served as the positive control inhibitor for ABCB1 and ABCG2, respectively. *p < 0.05, **p < 0.01 versus the control group.

expressions of ABCB1 of three specimens were detected by flow cytometry, and their expression rates were 63.7%, 40.6%, and 19.7%, respectively (Figure 2E). Every specimen was divided into four groups and were treated with saline, lazertinib, DOX, and combination therapy, respectively. The result of a representative case is shown in Figure 2F, and the quantifications of three cases are shown in Figure 2G, which indicated that DOX was resistant in the ABCB1-overexpressing specimens and that lazertinib was able to reverse the resistance of DOX effectively. The results suggested that lazertinib effectively enhanced the efficacy of the substrate drug in ABCB1-overexpressing human tumor specimens.

Lazertinib increased the cellular retention of ABCB1/ABCG2 substrate anticancer drugs in MDR cells by inhibiting drug efflux

The fluorescent compounds DOX and Rho 123, which are known substrates of ABCB1 and ABCG2, were used to evaluate the effect of lazertinib on drug accumulation and efflux assays. After a 3-h incubation with DOX or Rho 123, the cellular accumulations of the fluorescent dyes were evaluated in the presence or absence of lazertinib. Compared with the sensitive parental cells (HepG2 and S1), the higher expression of ABCB1 and ABCG2 in the MDR cells (HepG2/adr and S1-MI-80 cells, respectively) caused low intracellular accumulation of DOX (Figures 3A and 3C) and Rho 123 (Figures 3B and 3D). Intriguingly, lazertinib was found to significantly increase the cellular accumulation of DOX and Rho 123 in the resistant HepG2/adr cells (Figures 3A and 3B) and S1-MI-80 cells (Figures 3C and 3D) in a concentration-dependent manner. However, the accumulation of DOX or Rho 123 in the parental cells (HepG2 and S1) was not affected notably by lazertinib.

To further confirm whether the increased cellular accumulation of the transporter substrate drugs was caused by inhibition of the drug efflux function of ABCB1 and ABCG2, the intracellular retention of a fluorescent ABCB1/ABCG2 substrate dye Rho 123 was examined and evaluated at different time points in the presence of lazertinib. Compared with the lazertinib-incubated cells, the intracellular retention of Rho 123 in the no-treatment cells was remarkably reduced at all time-points in MDR cells. However, no significant alteration was observed in the parental HepG2 cells (Figure 3E) and S1 cells (Figure 3F). The results indicated that lazertinib increased cellular accumulation of ABCB1/ABCG2 substrate drugs in MDR cells by blocking the drug efflux function of the transporters.

Lazertinib stimulated the activity of ABCB1 and ABCG2 ATPase

To examine whether lazertinib affected the ATPase activity of the ABC transporters, the vanadate-sensitive ATPase activity of ABCB1/ABCG2 was detected in the presence of various concentrations of lazertinib. Lazertinib was found to stimulate the ATPase activity of both ABCB1 and ABCG2 in a concentration-dependent

Table 2. Effect of lazertinib on reversing the MDR mediated by ABCB1 or ABCG2 in stable transfected cells

Compounds	IC ₅₀ ± SD (μM) (fold reversal)			
	HEK293/vector		HEK293/ABCB1	
Doxorubicin	0.06088 ± 0.0098	(1.00)	1.2238 ± 0.1424	(1.00)
+0.0625 μM Lazertinib	0.05451 ± 0.0032	(1.11)	0.3212 ± 0.0124**	(3.81)
+0.125 μM Lazertinib	0.0720 ± 0.0012	(0.84)	0.2497 ± 0.0275**	(4.90)
+0.25 μM Lazertinib	0.0528 ± 0.0023	(1.15)	0.1073 ± 0.0129**	(11.40)
+10 μM Verapamil	0.06244 ± 0.0087	(0.97)	0.0692 ± 0.0044**	(17.68)
Paclitaxel	0.0157 ± 0.0033	(1.00)	2.7183 ± 0.0296	(1.00)
+0.0625 μM Lazertinib	0.0163 ± 0.0006	(0.96)	1.8755 ± 0.0109	(1.44)
+0.125 μM Lazertinib	0.0149 ± 0.0034	(1.05)	0.8179 ± 0.0130**	(3.32)
+0.25 μM Lazertinib	0.0182 ± 0.0025	(0.86)	0.3574 ± 0.0590**	(7.62)
+10 μM Verapamil	0.0145 ± 0.0013	(0.85)	0.1451 ± 0.0155**	(18.74)
Cisplatin	1.9158 ± 0.1223	(1.00)	3.3022 ± 0.6193	(1.00)
+0.25 μM Lazertinib	2.2725 ± 0.2337	(0.84)	3.2578 ± 0.6124	(1.01)
	HEK293/Vector		HEK293/ABCG2	
Mitoxantrone	0.0634 ± 0.0031	(1.00)	0.6514 ± 0.0663	(1.00)
+0.0625 μM Lazertinib	0.0567 ± 0.0046	(1.11)	0.2229 ± 0.0445*	(2.92)
+0.125 μM Lazertinib	0.0354 ± 0.0034	(1.79)	0.1258 ± 0.0207**	(5.17)
+0.25 μM Lazertinib	0.0410 ± 0.0061	(1.54)	0.0725 ± 0.0269**	(8.97)
+2.5 μM FTC	0.0461 ± 0.0035	(1.37)	0.0601 ± 0.0451**	(10.84)
Topotecan	0.0948 ± 0.0092	(1.00)	1.8948 ± 0.0508	(1.00)
+0.0625 μM Lazertinib	0.1133 ± 0.0089	(0.83)	1.4401 ± 0.0464	(1.31)
+0.125 μM Lazertinib	0.1193 ± 0.0071	(0.79)	0.2588 ± 0.0308**	(7.32)
+0.25 μM Lazertinib	0.1367 ± 0.0061	(0.69)	0.1587 ± 0.0154**	(11.94)
+2.5 μM FTC	0.1231 ± 0.0077	(0.77)	0.1052 ± 0.0400**	(18.00)
Cisplatin	1.9158 ± 0.1223	(1.00)	2.4612 ± 0.0566	(1.00)
+0.25 μM Lazertinib	2.2725 ± 0.2337	(0.84)	2.1443 ± 0.0491	(1.17)

The IC₅₀ of each drug was calculated by MTT assay, and the value represents means and SD of three independent results. Setting the ratio of the IC₅₀ for chemotherapeutic agent alone versus the IC₅₀ for combination with lazertinib as the fold reversal of MDR. VRP and FTC served as the positive control inhibitor for ABCB1 and ABCG2. *p < 0.05, **p < 0.01 versus the control group.

manner. The ATPase activity reached a plateau near 62 or 70 nmol/min/mg protein in ABCB1 (Figure 4A) or ABCG2 (Figure 4B), respectively, which was attained at 0.5/0.2 μM lazertinib. At higher concentration of lazertinib, the stimulated ABCB1/ABCG2 ATPase activity remained steady up to the highest concentration tested (1 μM). The results suggested that lazertinib could significantly enhance the ATPase activity of ABC transporters.

Lazertinib inhibited the photoaffinity labeling of ABCB1 and ABCG2

The photoaffinity analog of prazosin, ¹²⁵I-IAAP, which is a known substrate of ABCB1 and ABCG2, has been widely used to determine the binding regions of the ABC transporters that interact with substrates and inhibitors. Previous reports have shown that the substrates or inhibitors of ABCB1/ABCG2 can compete with ¹²⁵I-iodoarylazido-

prazosin (¹²⁵I-IAAP) for photolabeling of the transporter.³⁴ It was noteworthy that lazertinib concentration-dependently inhibited the photolabeling of ABCB1 (Figure 4C) and ABCG2 (Figure 4D), and their 50% inhibition concentrations of lazertinib were approximately 0.4 and 0.2 μM, respectively. Thus, lazertinib might compete with the ABCB1/ABCG2 substrates to bind to the substrate-binding sites of the transporter to mediate the decrease in efflux of the substrate drugs and the increase of the cellular drugs.

Lazertinib did not alter ABCB1 or ABCG2 expression and localization in the MDR cells

Since the alteration of ABC transporter expression might also contribute to the reversal of MDR,^{35,36} we further evaluated the effect of lazertinib on the mRNA and protein levels of ABCB1 or ABCG2 using PCR and western blot/flow cytometric analyses, respectively. After treatment with different concentrations of lazertinib or for different durations of time, there were no noticeable differences in ABCB1 or ABCG2 protein expression (Figure 5A). By quantitative real-time PCR, the mRNA expression of ABCB1 or ABCG2 was also not appreciably affected by lazertinib treatment in the MDR cells (Figures 5B and 5C). Moreover, lazertinib did not alter the plasma membrane localization of ABCB1 or ABCG2 in cancer cells according to the flow cytometry and immunofluorescence (Figures 5D–5F). The results suggested that the reversal of MDR by lazertinib is unrelated to the alteration of ABCB1 and ABCG2 expression.

ABCB1 or ABCG2 knockdown decreased the chemotherapy-sensitizing effect of lazertinib

To further determine the reversal efficacy of lazertinib mediated by ABCB1 or ABCG2, the cells with knockdown of *mdr1* or ABCG2 by shRNA were established. The knockdown efficacy was confirmed by western blotting (Figure 6A), and the cell growth rate was not changed by ABCB1 or ABCG2 protein expression level (Figure 6B). Then the effect of lazertinib on reversal of MDR was examined by MTT assay. Similarly, 0.25 μM lazertinib was chosen as the highest concentration used in the MDR reversal studies, because approximately 90% of cells remain viable after lazertinib treatment (Figure 6C). The results showed that the fold reversal of lazertinib was significantly reduced in the cells with knockdown of *mdr1* or ABCG2 compared with that in the overexpression of ABCB1 or ABCG2 parental cells (Table 3). These suggest that ABCB1 or ABCG2 knockdown decreases the efficacy of lazertinib on the reversal of MDR.

Lazertinib did not affect EGFR downstream signaling pathway at the MDR reversal drug concentration

As reported previously, the blockade of phosphorylation of kinases downstream of EGFR could also enhance the chemosensitivity of MDR cells to anticancer drugs.³⁷ To verify whether the MDR reversal concentrations of lazertinib could affect the Akt and Erk1/2 signaling pathway, western blots were performed. After lazertinib treatment at its MDR reversal concentrations, the expressions of total or phosphorylated Akt and Erk1/2 were not significantly changed in HepG2 (Figure 6D), HepG2/adr (Figure 6E), KB (Figure 6G),

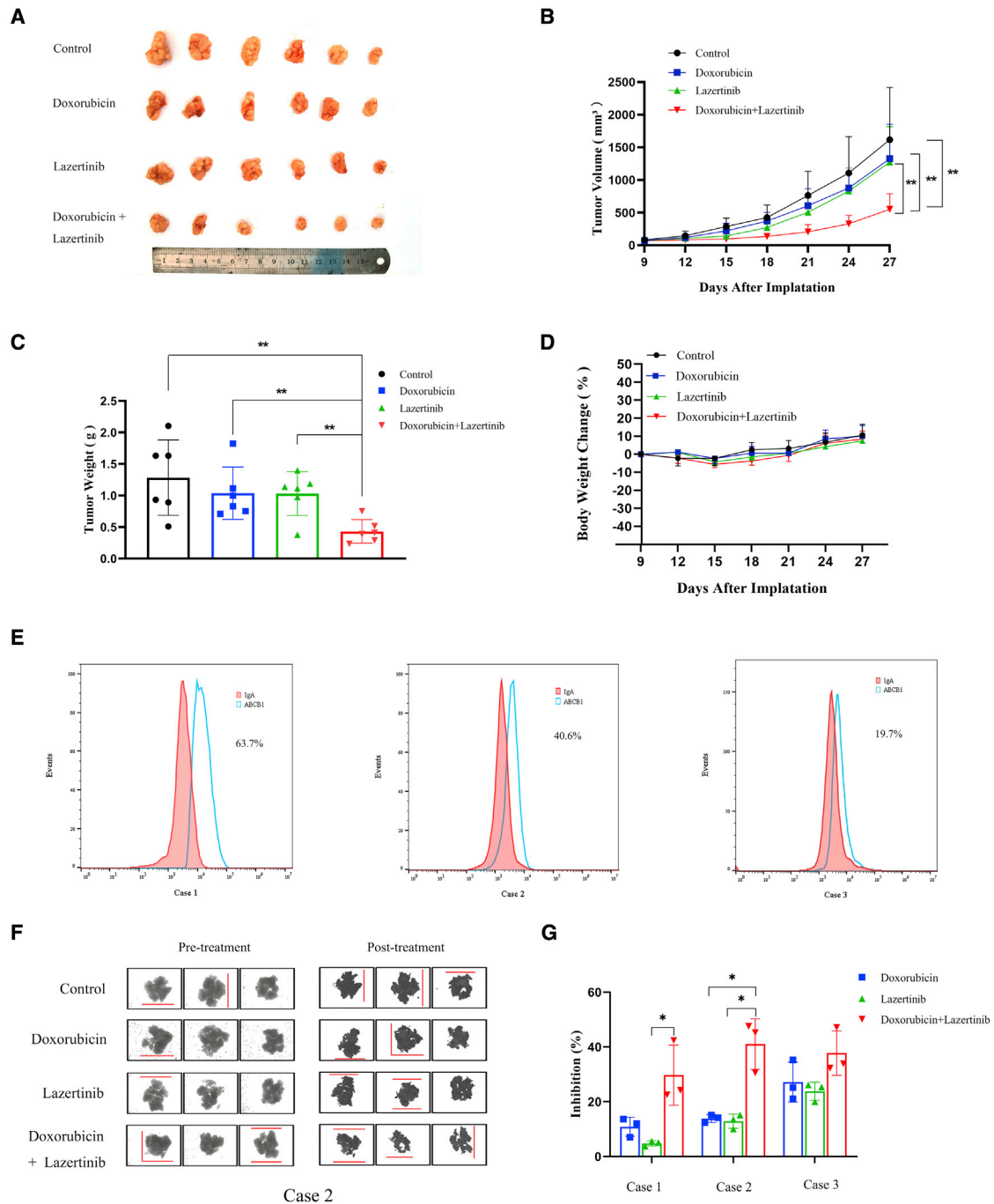
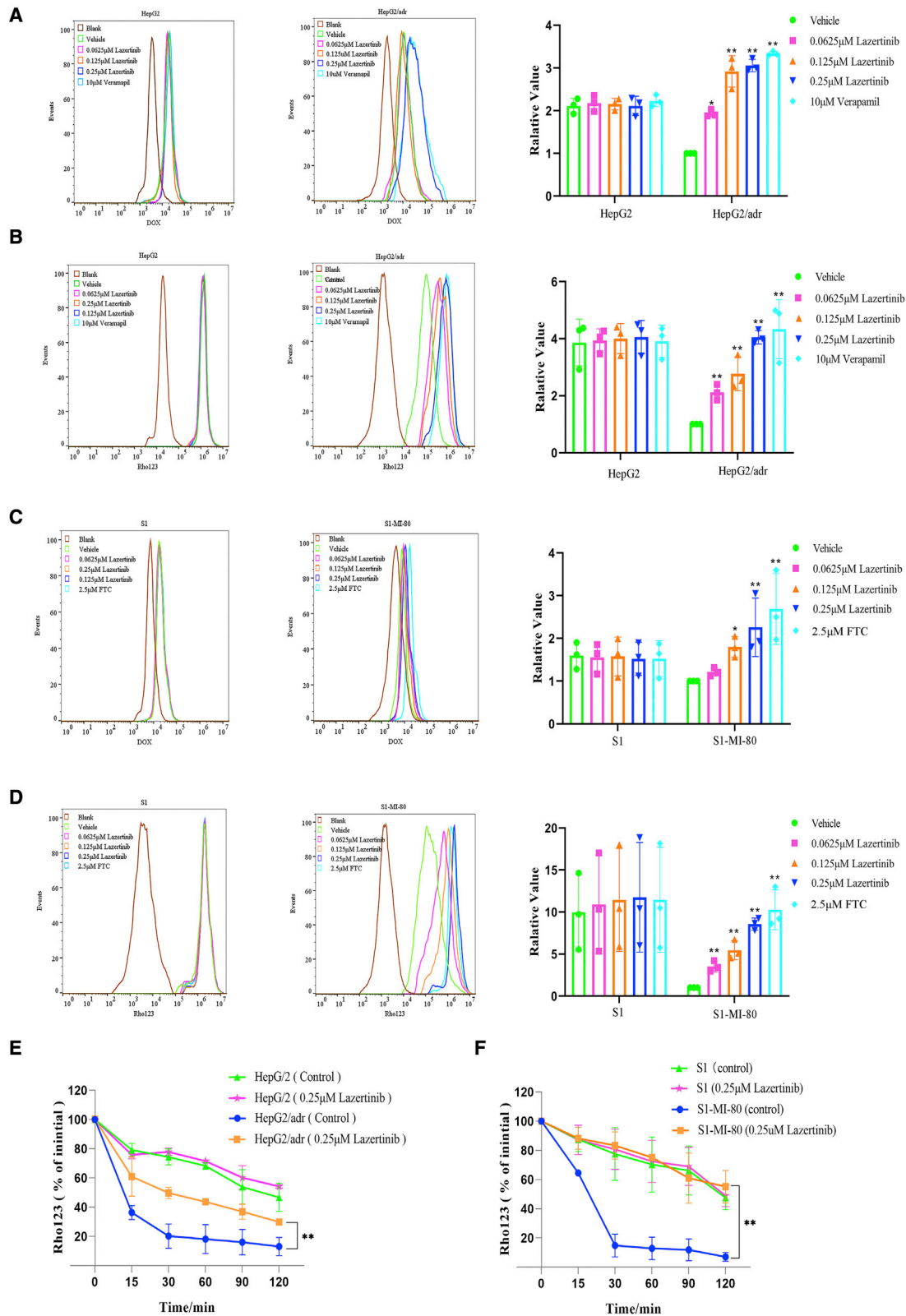


Figure 2. The MDR-reversing effect of lazertinib was evaluated in the ABCB1-overexpressing HepG2/adr tumor xenograft model *in vivo* and the ABCB1-overexpressing specimens *ex vivo*

(A) Photograph of resected tumor xenograft specimen at the end of the 28-day observation period is shown. The tumor growth curves of each treatment group were plotted. (B) Mean \pm SD of tumor volume in each treatment group is presented. (C) The bar chart represents the mean \pm SD tumor weight of each treatment group ($n = 6$). (D) Changes in mouse body weight after tumor xenograft inoculation. Mean \pm SD of per treatment group is presented. The different treatment groups are as follows: saline (q3dX6), doxorubicin (2 mg/kg i.p., q3dX6), lazertinib (10 mg/kg p.o., q3dX6), lazertinib (10 mg/kg p.o., q3dX6, given 1 h before doxorubicin treatment), and doxorubicin (2 mg/kg i.p., q3dX6). (E) The expression levels of ABCB1 of three clinical tumor specimens were examined using flow cytometric assay. (F) Representative images of *ex vivo* tumor specimens. Left: the specimens before drug treatment; right: living cells after drug treatment (MTT staining) captured by the system. (G) Inhibition percentages after different treatments of three specimens. The different treatment groups are as follows: saline; 2.3 μ g/mL doxorubicin alone, 1.6 μ g/mL lazertinib alone, combination of 1.6 μ g/mL lazertinib (given 1 h before treatment of doxorubicin) and 2.3 μ g/mL doxorubicin. ** $p < 0.01$, significantly different from the saline control group.



(legend on next page)

KBv200 (Figure 6H), S1 (Figure 6J), and S1-MI-80 cells (Figure 6K). The results suggested that the MDR reversal effect of lazertinib is independent of the inhibition of the EGFR signaling pathway.

DISCUSSION

The overexpression of ABC transporters in MDR cancer cells is a major hindrance to chemotherapy. With an aim to overcome MDR, numerous transporter inhibitors have been investigated.^{38–40} These modulators could be grouped into the following four categories. (1) First-generation modulators include tamoxifen, verapamil, and cyclosporin A. They are not effective to elicit MDR reversal *in vivo* due to unacceptable toxicity.⁴¹ (2) Second-generation modulators include S9788 and PSC833. They were found to cause significant pharmacokinetic alterations of concomitantly administered chemotherapeutic drugs and thus led to unpredictable side effects.²³ (3) Third-generation modulators (e.g., tariquidar [XR9576], zosuquidar, and GF120918) and fourth-generation modulators (e.g., neochamaejasmin B [NCB] and curcumin) are generally less toxic and cause less pharmacokinetic interaction with anticancer drugs. However, unsatisfactory outcomes from clinical trials have limited the clinical application of the third- and fourth-generation modulators.^{42–44} Therefore, novel and effective strategies for MDR reversal are still badly needed.

The development of TKIs as molecular targeted agents represents a breakthrough in cancer therapy. TKIs work by specifically binding to the ATP-binding site of oncogenic tyrosine kinases and thus selectively inhibit tumor growth. Interestingly, we and others have reported that numerous TKIs could also be used to reverse ABC transporter-mediated MDR.⁴⁵ TKIs were found to interact with the ATP-binding site of ABC transporters and inhibit the drug efflux function to circumvent MDR.^{45,46} On the other hand, some TKIs were also reported to downregulate the expression of ABC transporters to enhance the efficacy of anticancer drug.³⁵

In this study, lazertinib, a novel third-generation, irreversible, and mutant selective EGFR TKI, was evaluated for its MDR reversal activity *in vitro*, *in vivo*, and *ex vivo*. Lazertinib was found to specifically enhance the efficacy of chemotherapeutic drugs in MDR cells overexpressing with ABCB1 or ABCG2 because drug sensitivity of parental cells was not affected by lazertinib. Moreover, lazertinib did not affect the cytotoxicity of other anticancer drugs that are not ABCB1/ABCG2 substrates (such as cisplatin) (Figure 1, Tables 1, 2). Meanwhile, ABCB1 or ABCG2 knockdown decreased the reversal efficacy of lazertinib, which further indicated that the reversal efficacy of lazertinib was mediated by ABCB1 or ABCG2 (Table 3). More importantly, the combination of lazertinib and doxorubicin was also found to exhibit a remarkably higher anticancer effect than doxorubicin or

lazertinib alone in an ABCB1-overexpressing HepG2/adr tumor xenograft nude mouse model *in vivo* (Figure 2). Meanwhile, the clinical specimens were used to evaluate the clinical relevance of reversal efficacy, and the results suggested that lazertinib could enhance the efficacy of traditional chemotherapeutic drugs *ex vivo*, which could provide more reference for clinical application (Figure 2).

To investigate the mechanism of the MDR reversal by lazertinib, the intracellular accumulation of fluorescent ABCB1/ABCG2 substrate dyes or anticancer drugs was evaluated. Lazertinib was found to increase the intracellular accumulation of ABCB1/ABCG2 substrate anticancer drugs in MDR cells overexpressing the transporters by inhibition of drug efflux, but no effect was observed in drug-sensitive cells (Figure 3). Further investigations revealed that lazertinib inhibited the photolabeling of ABCB1 and ABCG2 by ¹²⁵I-IAAP. Therefore, lazertinib may interact with the substrate-binding sites of ABCB1/ABCG2 to inhibit the efflux function of the transporters in a competitive manner (Figure 4). Moreover, the stimulation of ABCB1 and ABCG2 ATPases by lazertinib is also consistent with the interaction of the TKI with the ATP-binding domain of the transporters. Therefore, the inhibition of drug efflux function of the transporters by lazertinib may be responsible for the observed MDR reversal. Some TKIs have been reported to downregulate the expression of ABC transporters to modulate MDR. In our study, lazertinib did not alter the expression of ABCB1 or ABCG2 at both mRNA and protein levels at concentrations up to 10 μ M, and the localization also did not change after the treatment of lazertinib (Figure 5). In addition, at the effective MDR reversal concentrations, lazertinib did not affect the EGFR downstream signaling pathway (Figure 6).

In summary, lazertinib was found to increase the cellular accumulation of transporters substrate chemotherapeutic drugs to modulate MDR by inhibiting the efflux function of ABCB1 or ABCG2 (Figure 7). Lazertinib may be adopted as a novel chemosensitizer to overcome MDR in ABCB1 or ABCG2-overexpressing cancer cells.

MATERIALS AND METHODS

Reagents and chemicals

Lazertinib was purchased from MedChemExpress (Princeton, NJ, USA). Vincristine (VCR), paclitaxel, DOX, mitoxantrone (MX), topotecan, G418, fumitremorgin C (FTC), verapamil (VRP), cisplatin, rhodamine 123 (Rho 123), and 1-(4,5-dimethylthiazol-2-yl)-3,5-diphenylformazan (MTT) were acquired from Sigma-Aldrich (St. Louis, MO, USA). Antibodies against ABCB1, ABCG2, ERK, and p-ERK, Akt, p-Akt, and flow cytometry antibodies against ABCG2 were obtained from Santa Cruz Biotechnology Inc. (Paso Robles, CA, USA). Glyceraldehyde-3-phosphate dehydrogenase (GAPDH) antibody was obtained from Kangchen Co. (Shanghai, China).

Figure 3. Effect of lazertinib on cellular accumulation and efflux of fluorescent substrates

The cellular retention of doxorubicin in (A) HepG2 and HepG2/adr; (C) S1 and S1-MI-80 and the cellular accumulation of Rho 123 in (B) HepG2 and HepG2/adr; (D) S1 and S1-MI-80 cells were measured, respectively. The Rho 123 efflux at different time points was detected in (E) HepG2 and HepG2/adr cells and (F) S1 and S1-MI-80 cells in the presence or absence of 0.25 μ M lazertinib. The relative values were estimated according to the fluorescence intensity in the MDR cells. All assays were repeated three times, and the data are expressed as means \pm SD. * $p < 0.05$, ** $p < 0.01$, significantly different from the control group.

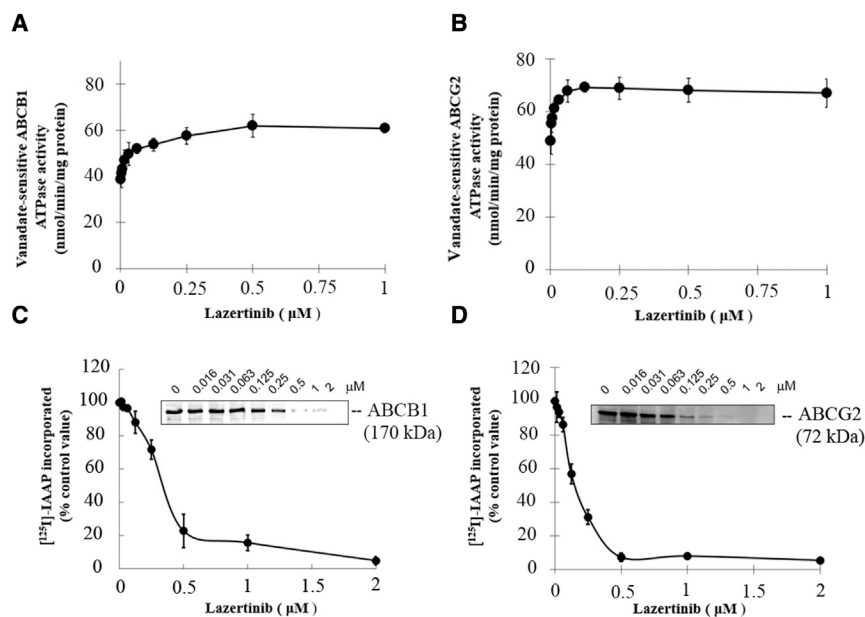


Figure 4. Effect of lazertinib on the ATPase activity and the ¹²⁵I-IAAP photolabeling of ABC transporters

(A and B) The ATPase activity of ABCB1 and ABCG2 was evaluated at the indicated concentrations of lazertinib. (C and D) Lazertinib competed for photolabeling of ABCB1 or ABCG2 by ¹²⁵I-IAAP. A representative autoradiogram from three independent experiments is shown. The relative amount of ¹²⁵I-IAAP incorporated is plotted against the concentration of lazertinib used in the incubation; 100% incorporation refers to the absence of lazertinib. The mean and standard error values from three independent experiments are shown.

ABCB1 and mouse IgG2b/κ antibodies used in flow cytometry were obtained from BD Biosciences (San Jose, CA, USA). RPMI 1640 and DMEM media were purchased from Thermo Fisher Scientific Inc. (Waltham, MA, USA). SYBR Green qPCR Master Mix was obtained from ExCell Bio (Shanghai, China).

Cell culture

The human hepatoma HepG2 (parental sensitive cells) and HepG2/adr cells (ABCB1-overexpressing drug-resistant cells); the colon carcinoma S1 (parental sensitive cells) and S1-M1-80 cells (ABCG2-overexpressing drug-resistant cells) were maintained in DMEM containing 10% fetal bovine serum (FBS). The RPMI 1640 medium supplemented with 10% FBS was used to culture the human oral carcinoma KB (parental sensitive) and KBv200 cells (ABCB1-overexpressing drug-resistant cells). To sustain the drug-resistance phenotype, all resistant cells were cultured in the presence of a selected drug at low concentration. At 2–3 weeks before experiments, resistant cells were allowed to grow in drug-free medium. HEK293 cells and their stable-transfected sub-lines (backbone vector, ABCB1, or ABCG2) were maintained in DMEM with 10% FBS and 100 μg/mL G418.

Cell proliferation and cytotoxicity assay

MTT assay was used to evaluate the cell proliferation and drug cytotoxicity as previously described.⁴⁷ The 50% inhibitory concentration (IC₅₀) was calculated by the Bliss method from the cell survival curves.⁴⁷ The resistance index (RI) of MDR cells and fold reversal by lazertinib were calculated with the following formula: RI = IC₅₀ of drugs in drug-resistant cells/IC₅₀ of drugs in the drug-sensitive cells; fold reversal = IC₅₀ of the conventional anticancer drug alone/IC₅₀ of the conventional anticancer drug when used in combination with lazertinib.

Animal experiment

HepG2/adr cell xenograft nude mouse model was established for the *in vivo* experiment as previously described.⁴⁸ Briefly, athymic nude mice (4–6 weeks of age and 16–20 g in weight) were subcutaneously inoculated with 1.0 × 10⁷ HepG2/adr cells. When average tumor volume reached 50 mm³, four groups of six mice each were randomized to receive the following treatment: (a) saline (q3d×6), (b) DOX alone (2 mg/kg i.p., q3d×6), (c) lazertinib alone (10 mg/kg p.o., q3d×6), or (d) combination of lazertinib (10 mg/kg p.o., q3d×6, given 1 h before treatment of DOX) and DOX (2 mg/kg i.p., q3d×6). The tumor sizes and mouse body weights were recorded every 3 days. Tumor volume (V) was estimated according to the following formula: $V = (\pi/6) [(A + B)/2]^3$ (A represents the maximal diameter, and B represents the perpendicular diameter). At the termination of the experiment, the mice were euthanized, and the tumors were stripped and weighed. The tumor inhibition rates (IR) were then calculated using the following formula:²⁷

$$IR(\%) = \left(1 - \frac{\text{Average tumor weight of treatment mouse}}{\text{Average tumor weight of control mouse}}\right) \times 100\%$$

Ethical approval for the animal experiment was granted by the Animal Ethics Committee of Sun Yat-sen University Cancer Center (No. L102042020090S).

Ex-vivo experiment

To evaluate the *ex vivo* reversal efficacy of lazertinib, an histoculture drug response assay was carried out according to a previous paper.⁴⁹ The tumor specimens were collected from patients that were diagnosed with hepatocellular carcinoma, and the specimens were placed in DMEM after the resection and were processed within 6 h.

First, the specimens were dissected into small pieces (1 × 1 × 1 mm³) and placed on filter-papers which were put on the scaffold of 24-well plates in 2 mL of medium. The sample volumes were calculated by the Image Analysis System to obtain the A-score. Then, the specimens were divided into four groups and given the following administrations for 3 days: (a) saline; (b) 2.3 μg/mL DOX alone; (c) 1.6 μg/mL lazertinib

alone, or (d) the combination of 1.6 $\mu\text{g}/\text{mL}$ lazertinib (given 1 h before treatment of DOX) and 2.3 $\mu\text{g}/\text{mL}$ DOX. After adding the MTT into the medium for 4 h, the stained area and intensity were determined by using the Image Analysis System to obtain the B-score. Finally, the inhibition rates (IR) were calculated using the following formula:

$$IR(\%) = \left(1 - \frac{\text{Average of B - Scores of treated samples} / \text{Average of A - Scores of treated samples}}{\text{Average of B - Scores of Control} / \text{Average of A - Scores of Control}} \right) \times 100\%$$

Ethical approval for the experiment was granted by the Zhujiang Hospital, Southern Medical University. (No.2021-KY-162-02)

DOX and Rho 123 accumulation assay

The accumulation of fluorescent ABCB1/ABCG2 probe substrates (i.e., DOX and Rho 123) in cells was analyzed with flow cytometry to indicate the inhibitory effect of the transporters by lazertinib, as previously described.⁵⁰ First, the cells were incubated with lazertinib at various concentrations for 3 h. Then, the medium containing 5 μM Rho 123 or 10 μM DOX was replaced to culture for 0.5 or 3 h, respectively. Afterward, the cells were collected and washed three times with ice-cold PBS. The drug accumulation was determined by flow cytometry. Verapamil and fumitremorgin C served as positive modulator control of ABCB1 and ABCG2, respectively.⁵¹

Rho 123 efflux assay

The drug efflux assays were carried out as described previously.⁵² Briefly, cells were first allowed to incubate in medium containing 5 μM of the fluorescent transporter substrate (Rho 123) for 30 min. The cells were then washed three times with ice-cold PBS. Afterward, the cells were maintained in fresh medium with or without 0.25 μM lazertinib, and the incubation continued. At different time points, the cells were collected and washed with ice-cold PBS, and the fluorescence intensity retained inside the cells was immediately analyzed by flow cytometric analysis.

ATPase assay of ABCB1 and ABCG2

The ATPase assay was carried out to measure the vanadate-sensitive ATPase activity of ABCB1 or ABCG2 in cell membrane prepared from High-Five insect cells (cat. no. 453270) using the BD Gentest ATPase assay kit (BD Biosciences, San Jose, CA, USA).⁵³ Briefly, ABCB1- or ABCG2-overexpressing cell membrane (100 $\mu\text{g}/\text{mL}$ protein) was incubated with lazertinib (0.001–1 μM) in a buffer of ATPase assay containing, or not, sodium orthovanadate (1.2 mM) at 37°C for 5 min. Then, 12 mM Mg-ATP was added into the total reaction volume to initiate the reaction of ATPase hydrolysis and adding 30 μL 10% sodium dodecyl sulfate (SDS) solution to terminate the reactions after 10 min at 37°C. Finally, measuring the absorbance at 800 nm was measured and quantitated using a phosphate standard curve to determine the inorganic phosphate release.

The photolabeling assay of ABCB1 and ABCG2 with ¹²⁵I-IAAP

Crude membrane from ABCB1- or ABCG2-overexpressing High Five insect cells (50 μg protein) was put together with 0–2 μM lazertinib for 5 min at normal temperature in 50 mM Tris-HCl (pH 7.5). Cross-linking was performed under ultraviolet (UV) light with 365-nm wavelength on ice after incubation with the ¹²⁵I-IAAP (3 nM, 2,200

Ci/nmol) under weak light for another 5 min. The photolabeled ABCB1 or ABCG2 was immunoprecipitated using the specific antibodies C219 (Enzo Life Sciences, Farmingdale, NY, USA) and BXP21 (Novus Biologicals, Centennial, CO, USA), respectively. Tris-acetate NuPAGE gel (7%) served as the loading of the sample in the SDS-polyacrylamide gel electrophoresis (SDS-PAGE) and then the gel was exposed under Bio-Max MR film for overnight at –80°C after being dried. The Storm 860 PhosphorImager system was used to quantify the incorporated radioactivity.

Western blot analysis

Western blot analysis was performed as described previously.³⁴ Briefly, the cells were treated with a range of different concentrations of lazertinib for different periods of time. Afterward, the cells were harvested, and the proteins of interest were separated by SDS-PAGE and detected with specific antibodies.

Quantitative real-time PCR

To evaluate the mRNA levels of ABCB1 and ABCG2, quantitative PCR analysis was carried out as previously described.⁵⁴ Briefly, the cells were treated with a range of different concentrations of lazertinib for various periods of time. Total RNA was then harvested and subjected to real-time PCR analysis. The PCR primers were 5'-GAGTCAAGG ATTTGGTCGT-3' (forward) and 5'-GATCTCGCT CCTGGAAG ATG-3' (reverse) for GAPDH, 5'-CAGGCTTGCTGTA ATTACCC A-3' (forward) and 5'-TCAAAGAAACAACGGTTCGG-3' (reverse) for ABCB1; 5'-TGGCTGTCATGGCTTCAGTA-3' (forward) and 5'-GCCACGTGATTCTCCACAA-3' (reverse) for ABCG2. SYBR Green qPCR Master Mix was used to conduct the qPCR assay. ΔC_T was calculated by subtracting the C_T of GAPDH from the C_T of the transcript under investigation (i.e., ABCB1 or ABCG2). Fold difference in gene expression was calculated by the $2^{-\Delta\Delta C_T}$ method.

Flow cytometry

Flow cytometric analysis was carried out to examine the expression of ABCB1 or ABCG2 on cell surface, as described previously.³⁰ Cells were incubated with various concentrations of lazertinib for 48 h. After a washing with PBS, the cells in suspension were incubated in the dark for 30 min with specific ABCB1/ABCG2 antibodies carrying a fluorescence tag. Cell samples incubated with an antibody against mouse IgG2b/ κ was used as the background control. Detection of

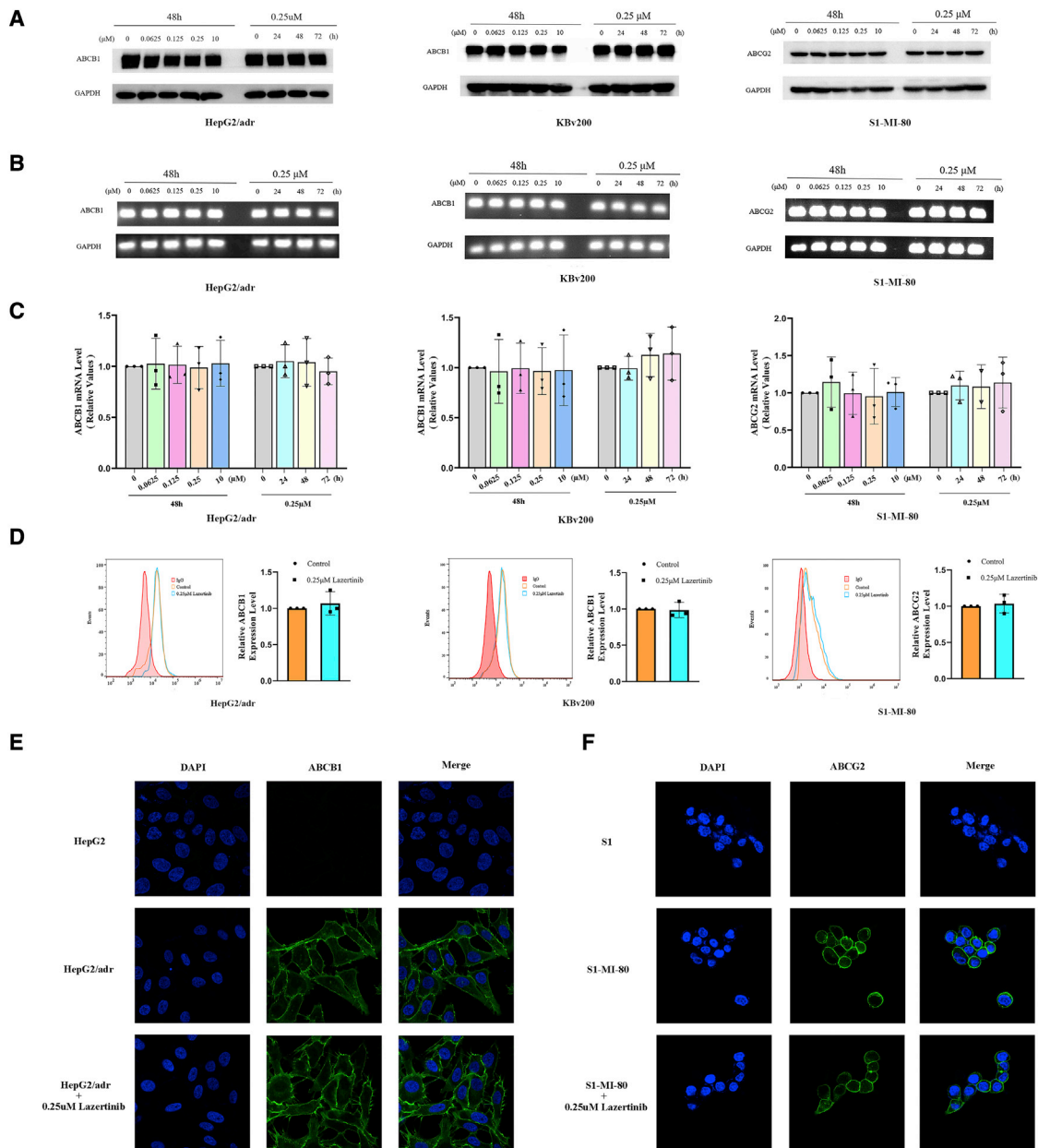


Figure 5. Effect of lazertinib on ABCB1 or ABCG2 expression of MDR cells

(A and B) The protein and mRNA expressions of ABCB1 and ABCG2 in MDR cells were examined by western blot and semi-quantitative RT-PCR assays, respectively. (C) The mRNA expression of ABCB1 and ABCG2 in the MDR cells were evaluated by real-time qPCR assay. (D) Protein expression of ABCB1 and ABCG2 on cell surface of MDR cells was examined using flow cytometric assay. (E and F) HepG2/adr cells and SI-MI-80 cells were treated with or without lazertinib at 0.25 μ M for 48 h. The subcellular localization pattern of ABCB1 or ABCG2 was evaluated using confocal laser scanning microscopy. ABCB1 or ABCG2 (green) and nuclei (DAPI, blue) were visualized. Means \pm SD of three independent experiments are shown.

fluorescence signal on cell surface by flow cytometry indicated the expression of the expression of the transporters.

Immunofluorescence

Cells were cultured in glass-bottomed confocal culture dishes and were treated with 0.25 μ M lazertinib for 48 h, and then the cells were fixed

with paraformaldehyde for 15 min after being washed three times with PBS. 0.1% Triton X-100 was used to permeabilize the membranes and 1% BSA was then used to blocked them. The primary antibody was incubated overnight, and then the secondary antibody was incubated for 1 h. Finally, the nucleus was stained with DAPI, and a Zeiss LSM 880 confocal microscope was used to acquire the images.

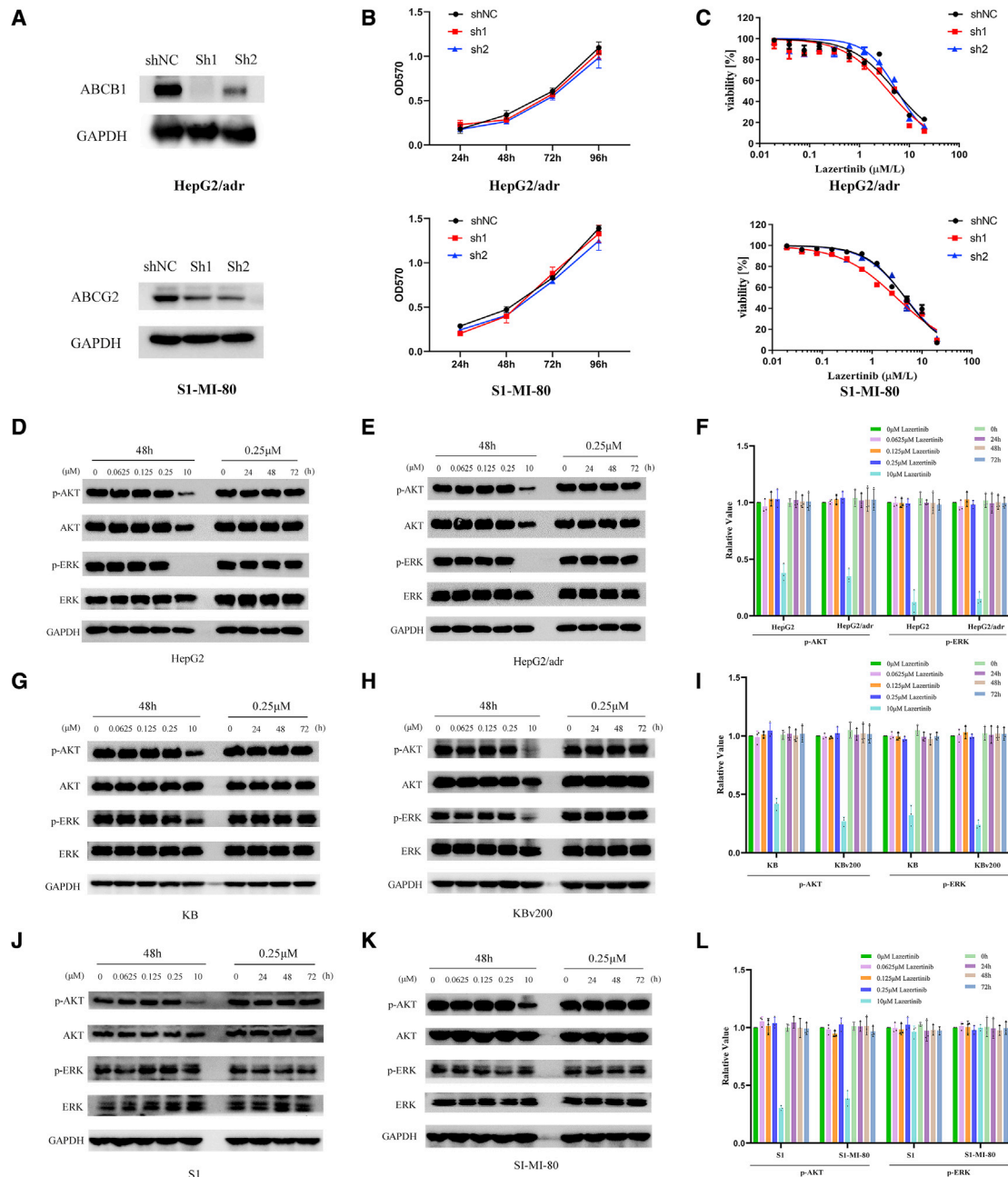


Figure 6. The knockdown efficacy of ABCB1 or ABCG2 and MTT cell growth curve and cytotoxicity of knockdown cells, the effect of lazertinib on the downstream signal pathway of EGFR

(A) Western blotting showing ABCB1 and ABCG2 knockdown in HepG2/adr cells and S1-MI-80 cells. (B and C) Cell growth curve and cytotoxicity of lazertinib alone were evaluated using the MTT assay in knockdown cells. Western blot analysis was used to detect the relative protein levels of Akt and ERK1/2 in HepG2 (D), HepG2/adr (E), KB (G), KBv200 (H), S1 (J), and S1-MI-80 (K) cells. Lazertinib (10 μ M) was used as the positive control, which blocked the activation of Akt and ERK1/2 in the cells. (F, I, and L) The protein levels of p-Akt and p-ERK were quantified. Representative blot images are shown from three independent experiments.

ABCB1 or ABCG2 knockdown assay

ABCB1- or ABCG2-specific shRNA were designed according to the genetic sequence of the National Center for Biotechnology Information (NCBI) database. The target sequences are as follows: ABCB1-

sh1: GAGGAGCAAAGAAGAAGAACT; ABCB1-sh2: GCAGAG AGGCAATCTTTAATCTC; ABCG2-sh1: GCAGATGCCTTCTT CGTTATG; ABCG2-sh2: GCTTCAGTACTTCAGCATTC. The shRNAs expressing pLKO.1 vector were co-transfected with psPAX2

Table 3. Effect of lazertinib on reversing the MDR mediated by ABCB1 or ABCG2 in knockdown cells

Compounds	IC ₅₀ ± SD (μM) (fold reversal)					
	HepG2/adr-ABCB1 shNC		HepG2/adr-ABCB1 sh1		HepG2/adr-ABCB1 sh2	
Doxorubicin	27.4661 ± 0.3836	(1.00)	4.0923 ± 0.0212	(1.00)	8.1376 ± 0.3808	(1.00)
+0.0625 μM Lazertinib	6.0025 ± 0.6877**	(4.57)	2.7734 ± 0.0282	(1.47)	6.9584 ± 1.4490	(1.17)
+0.125 μM Lazertinib	2.1431 ± 0.0423**	(12.81)	2.8496 ± 0.0486	(1.43)	4.4796 ± 0.1982	(1.82)
+0.25 μM Lazertinib	1.9838 ± 0.0659**	(13.84)	2.2005 ± 0.0195	(1.85)	3.6996 ± 0.0653**	(2.19)
+10 μM Verapamil	1.7909 ± 0.0757**	(15.34)	0.9553 ± 0.0224**	(4.28)	3.0630 ± 0.0742**	(2.66)
Paclitaxel	5.3889 ± 1.3112	(1.00)	0.6308 ± 0.0622	(1.00)	0.8578 ± 0.0114	(1.00)
+0.0625 μM Lazertinib	1.8651 ± 0.4068	(2.89)	0.6617 ± 0.0561	(0.98)	0.6030 ± 0.0072	(1.42)
+0.125 μM Lazertinib	0.5911 ± 0.0557**	(9.12)	0.4907 ± 0.0152	(1.35)	0.5427 ± 0.0083	(1.58)
+0.25 μM Lazertinib	0.6033 ± 0.1084**	(8.94)	0.3140 ± 0.0161	(2.11)	0.4432 ± 0.0067	(1.93)
+10 μM Verapamil	0.4287 ± 0.3642**	(12.56)	0.2201 ± 0.0354**	(3.01)	0.1989 ± 0.0045**	(4.31)
Cisplatin	3.0031 ± 0.0559	(1.00)	2.0149 ± 0.3111	(1.00)	3.3798 ± 0.2410	(1.00)
+0.25 μM Lazertinib	3.4615 ± 0.0913	(0.86)	2.2279 ± 0.5146	(0.90)	3.7883 ± 0.2290	(0.89)
	S1-MI-80-ABCG2 shNC		S1-MI-80-ABCG2-sh1		S1-MI-80-ABCG2 sh2	
Mitoxantrone	6.5865 ± 0.0648	(1.00)	0.8174 ± 0.0769	(1.00)	0.8344 ± 0.0164	(1.00)
+0.0625 μM Lazertinib	3.0584 ± 0.0161	(2.15)	0.4375 ± 0.0042	(1.86)	0.3831 ± 0.0287	(2.17)
+0.125 μM Lazertinib	1.2227 ± 0.0035**	(5.39)	0.1650 ± 0.0025**	(4.95)	0.1917 ± 0.0078**	(4.23)
+0.25 μM Lazertinib	0.6506 ± 0.0093**	(10.12)	0.1561 ± 0.0056**	(5.23)	0.1403 ± 0.0012**	(5.94)
+2.5 μM FTC	0.2994 ± 0.0039**	(21.98)	0.1059 ± 0.0049**	(7.71)	0.1073 ± 0.0012**	(7.77)
Topotecan	5.9804 ± 0.4179	(1.00)	0.6302 ± 0.0776	(1.00)	0.4415 ± 0.0283	(1.00)
+0.0625 μM Lazertinib	1.2441 ± 0.1245**	(4.81)	0.7606 ± 0.0457	(0.83)	0.1148 ± 0.0524	(3.84)
+0.125 μM Lazertinib	0.7135 ± 0.1281**	(8.38)	0.2933 ± 0.0124	(2.15)	0.1203 ± 0.0356*	(3.67)
+0.25 μM Lazertinib	0.5502 ± 0.0864**	(10.87)	0.2536 ± 0.0049	(2.48)	0.2195 ± 0.0362	(2.01)
+2.5 μM FTC	0.4633 ± 0.1040**	(12.91)	0.3612 ± 0.0819	(1.47)	0.1020 ± 0.0138*	(4.32)
Cisplatin	5.7041 ± 0.1271	(1.00)	3.7557 ± 0.0172	(1.00)	4.7405 ± 0.2325	(1.00)
+0.25 μM Lazertinib	4.8578 ± 0.0689	(1.17)	5.2267 ± 0.0334	(0.72)	5.6188 ± 0.0539	(0.84)

The IC₅₀ of each drug was calculated by MTT assay, and the value represents means and SD of three independent results. Setting the ratio of the IC₅₀ for chemotherapeutic agent alone versus the IC₅₀ for combination with lazertinib as the fold reversal of MDR. VRP and FTC served as the positive control inhibitor for ABCB1 and ABCG2. *P < 0.05, **P < 0.01 versus the shNC group.

and pMD.2G into 293 T cells by lentiviral infection. Viral supernatant was collected after the transfection for 72 h, filtered, and added to the culture medium of cancer cells for 24 h. Then, the cancer cells were treated with puromycin (5 μg/mL) after 48 h. Knockdown efficacy was confirmed by western blotting.

Statistical analysis

All experiments were repeated three times. Statistical significance was determined by Student's t test. All results are presented as means ± standard deviations. Significance was set at *p < 0.05, **p < 0.01.

ACKNOWLEDGMENTS

We would like to thank Dr. Susan Bates (Columbia University, New York, NY, USA) for the S1 parental and S1-MI-80 ABCG2-overexpressing colon cancer cell lines. This work was supported by grants

from National Science and Technology Major Project “Key New Drug Creation and Manufacturing Program” (No. 2018ZX09711002), Natural Scientific Foundation of China (No. 82073882, No. 82073317), The Guangdong Provincial Special Fund for Marine Economic Development Project (No. GDNRC [2020] 042).

AUTHOR CONTRIBUTIONS

L.W.F. and Y.F.F. designed experiments and supervised the study. T.T., Z.X.G., K.K.T., D.C., S.C.W., and M.L. performed experiments and processed data. C.Y., J.S.L., and F.W. contributed to organizing data and constructing databases.

DECLARATION OF INTEREST

The authors have no relevant competing interests to declare.

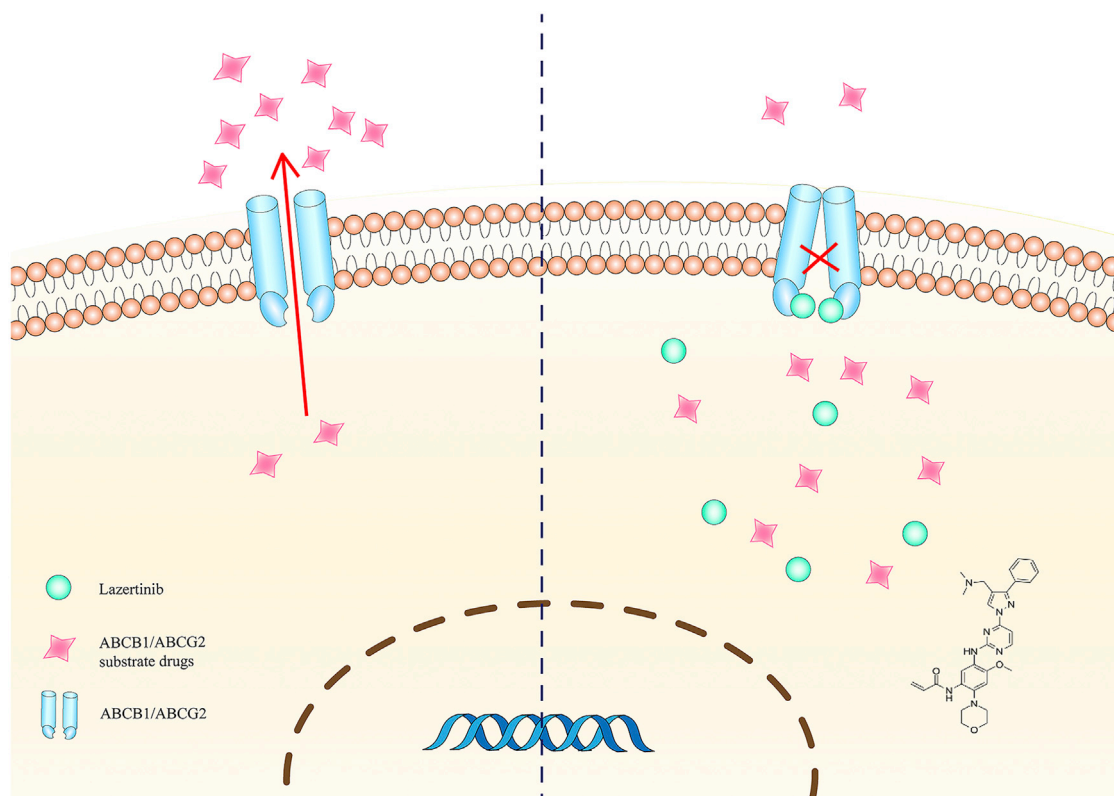


Figure 7. A schematic diagram illustrating the proposed mechanism contributing to MDR reversal by lazertinib

Left: In the absence of MDR inhibitor, ABCB1/ABCG2 substrate anticancer drugs are effectively pumped out of MDR cells, leading to low intracellular drug concentration and resistance. Right: Lazertinib inhibits the drug efflux function of ABCB1/ABCG2 to increase drug accumulation in MDR cells and circumvent drug resistance.

REFERENCES

1. Fojo, A., Hamilton, T.C., Young, R.C., and Ozols, R.F. (1987). Multidrug resistance in ovarian cancer. *Cancer* 60, 2075–2080.
2. Gottesman, M.M., Lavi, O., Hall, M.D., and Gillet, J.P. (2016). Toward a better understanding of the complexity of cancer drug resistance. *Annu. Rev. Pharmacol. Toxicol.* 56, 85–102.
3. Wu, Q., Yang, Z., Nie, Y., Shi, Y., and Fan, D. (2014). Multi-drug resistance in cancer chemotherapeutics: mechanisms and lab approaches. *Cancer Lett.* 347, 159–166.
4. Zhang, H., Huang, L., Tao, L., Zhang, J., Wang, F., Zhang, X., and Fu, L. (2019). Secalonic acid D induces cell apoptosis in both sensitive and ABCG2-overexpressing multidrug resistant cancer cells through upregulating c-Jun expression. *Acta Pharm. Sin B* 9, 516–525.
5. Lage, H. (2008). An overview of cancer multidrug resistance: a still unsolved problem. *Cell Mol Life Sci.* 65, 3145–3167.
6. Goldman, B. (2003). Multidrug resistance: can new drugs help chemotherapy score against cancer? *J. Natl. Cancer Inst.* 95, 255–257.
7. Zhang, Y.K., Wang, Y.J., Gupta, P., and Chen, Z.S. (2015). Multidrug resistance proteins (MRPs) and cancer therapy. *Aaps j* 17, 802–812.
8. Gottesman, M.M., Fojo, T., and Bates, S.E. (2002). Multidrug resistance in cancer: role of ATP-dependent transporters. *Nat. Rev. Cancer* 2, 48–58.
9. Wu, S., Luo, M., To, K.K.W., Zhang, J., Su, C., Zhang, H., An, S., Wang, F., Chen, D., and Fu, L. (2021). Intercellular transfer of exosomal wild type EGFR triggers osimertinib resistance in non-small cell lung cancer. *Mol. Cancer* 20, 17.
10. Xu, M., Wang, F., Li, G., Wang, X., Fang, X., Jin, H., Chen, Z., Zhang, J., and Fu, L. (2019). MED12 exerts an emerging role in actin-mediated cytokinesis via LIMK2/cofilin pathway in NSCLC. *Mol. Cancer* 18, 93.
11. Dean, M., Hamon, Y., and Chimini, G. (2001). The human ATP-binding cassette (ABC) transporter superfamily. *J. Lipid Res.* 42, 1007–1017.
12. Chen, Z., Shi, T., Zhang, L., Zhu, P., Deng, M., Huang, C., Hu, T., Jiang, L., and Li, J. (2016). Mammalian drug efflux transporters of the ATP binding cassette (ABC) family in multidrug resistance: a review of the past decade. *Cancer Lett.* 370, 153–164.
13. Liu, F.S. (2009). Mechanisms of chemotherapeutic drug resistance in cancer therapy—a quick review. *Taiwan J. Obstet. Gynecol.* 48, 239–244.
14. Gillet, J.P., Efferth, T., and Remacle, J. (2007). Chemotherapy-induced resistance by ATP-binding cassette transporter genes. *Biochim. Biophys. Acta* 1775, 237–262.
15. Borst, P., and Elferink, R.O. (2002). Mammalian ABC transporters in health and disease. *Annu. Rev. Biochem.* 71, 537–592.
16. Juliano, R.L., and Ling, V. (1976). A surface glycoprotein modulating drug permeability in Chinese hamster ovary cell mutants. *Biochim. Biophys. Acta* 455, 152–162.
17. Schinkel, A.H., Mol, C.A., Wagenaar, E., van Deemter, L., Smit, J.J., and Borst, P. (1995). Multidrug resistance and the role of P-glycoprotein knockout mice. *Eur. J. Cancer* 31a, 1295–1298.
18. Takenaka, K., Morgan, J.A., Scheffer, G.L., Adachi, M., Stewart, C.F., Sun, D., Leggas, M., Ejendal, K.F., Hrycyna, C.A., and Schuetz, J.D. (2007). Substrate overlap between Mrp4 and Abcg2/Bcrp affects purine analogue drug cytotoxicity and tissue distribution. *Cancer Res.* 67, 6965–6972.

19. Jonker, J.W., Smit, J.W., Brinkhuis, R.F., Maliepaard, M., Beijnen, J.H., Schellens, J.H., and Schinkel, A.H. (2000). Role of breast cancer resistance protein in the bioavailability and fetal penetration of topotecan. *J. Natl. Cancer Inst.* *92*, 1651–1656.
20. Sabnis, N.G., Miller, A., Titus, M.A., and Huss, W.J. (2017). The efflux transporter ABCG2 maintains prostate stem cells. *Mol. Cancer Res.* *15*, 128–140.
21. Li-Blatter, X., Beck, A., and Seelig, A. (2012). P-glycoprotein-ATPase modulation: the molecular mechanisms. *Biophys. J.* *102*, 1383–1393.
22. Szakács, G., Paterson, J.K., Ludwig, J.A., Booth-Genthe, C., and Gottesman, M.M. (2006). Targeting multidrug resistance in cancer. *Nat. Rev. Drug Discov.* *5*, 219–234.
23. Coley, H.M. (2010). Overcoming multidrug resistance in cancer: clinical studies of p-glycoprotein inhibitors. *Methods Mol. Biol.* *596*, 341–358.
24. Huang, L., Jiang, S., and Shi, Y. (2020). Tyrosine kinase inhibitors for solid tumors in the past 20 years (2001–2020). *J. Hematol. Oncol.* *13*, 143.
25. Zeng, F., Wang, F., Zheng, Z., Chen, Z., Wah To, K.K., Zhang, H., Han, Q., and Fu, L. (2020). Rociletinib (CO-1686) enhanced the efficacy of chemotherapeutic agents in ABCG2-overexpressing cancer cells in vitro and in vivo. *Acta Pharm. Sin B* *10*, 799–811.
26. Yang, K., Chen, Y., To, K.K., Wang, F., Li, D., Chen, L., and Fu, L. (2017). Alecetinib (CH5424802) antagonizes ABCB1- and ABCG2-mediated multidrug resistance in vitro, in vivo and ex vivo. *Exp. Mol. Med.* *49*, e303.
27. Wang, X.K., To, K.K., Huang, L.Y., Xu, J.H., Yang, K., Wang, F., Huang, Z.C., Ye, S., and Fu, L.W. (2014). Afatinib circumvents multidrug resistance via dually inhibiting ATP binding cassette subfamily G member 2 in vitro and in vivo. *Oncotarget* *5*, 11971–11985.
28. Chen, Z., Chen, Y., Xu, M., Chen, L., Zhang, X., To, K.K., Zhao, H., Wang, F., Xia, Z., Chen, X., et al. (2016). Osimertinib (AZD9291) enhanced the efficacy of chemotherapeutic agents in ABCB1- and ABCG2-overexpressing cells in vitro, in vivo, and ex vivo. *Mol. Cancer Ther.* *15*, 1845–1858.
29. Ma, S.L., Hu, Y.P., Wang, F., Huang, Z.C., Chen, Y.F., Wang, X.K., and Fu, L.W. (2014). Lapatinib antagonizes multidrug resistance-associated protein 1-mediated multidrug resistance by inhibiting its transport function. *Mol. Med.* *20*, 390–399.
30. Wang, F., Li, D., Zheng, Z., Kin Wah To, K., Chen, Z., Zhong, M., Su, X., Chen, L., and Fu, L. (2020). Reversal of ABCB1-related multidrug resistance by ERK5-IN-1. *J. Exp. Clin. Cancer Res.* *39*, 50.
31. Xu, L., Huang, J., Liu, J., Xi, Y., Zheng, Z., To, K.K.W., Chen, Z., Wang, F., Zhang, Y., and Fu, L. (2020). CM082 enhances the efficacy of chemotherapeutic drugs by inhibiting the drug efflux function of ABCG2. *Mol. Ther. Oncolytics* *16*, 100–110.
32. Yun, J., Hong, M.H., Kim, S.Y., Park, C.W., Kim, S., Yun, M.R., Kang, H.N., Pyo, K.H., Lee, S.S., Koh, J.S., et al. (2019). YH25448, an irreversible EGFR-TKI with potent intracranial activity in EGFR mutant non-small cell lung cancer. *Clin. Cancer Res.* *25*, 2575–2587.
33. Ahn, M.J., Han, J.Y., Lee, K.H., Kim, S.W., Kim, D.W., Lee, Y.G., Cho, E.K., Kim, J.H., Lee, G.W., Lee, J.S., et al. (2019). Lazertinib in patients with EGFR mutation-positive advanced non-small-cell lung cancer: results from the dose escalation and dose expansion parts of a first-in-human, open-label, multicentre, phase 1-2 study. *Lancet Oncol.* *20*, 1681–1690.
34. Tong, X.Z., Wang, F., Liang, S., Zhang, X., He, J.H., Chen, X.G., Liang, Y.J., Mi, Y.J., To, K.K., and Fu, L.W. (2012). Apatinib (YN968D1) enhances the efficacy of conventional chemotherapeutic drugs in side population cells and ABCB1-overexpressing leukemia cells. *Biochem. Pharmacol.* *83*, 586–597.
35. Hoffmann, K., Shibo, L., Xiao, Z., Longerich, T., Büchler, M.W., and Schemmer, P. (2011). Correlation of gene expression of ATP-binding cassette protein and tyrosine kinase signaling pathway in patients with hepatocellular carcinoma. *Anticancer Res.* *31*, 3883–3890.
36. Huang, Y.S., Xue, Z., and Zhang, H. (2015). Sorafenib reverses resistance of gastric cancer to treatment by cisplatin through down-regulating MDR1 expression. *Med. Oncol.* *32*, 470.
37. Goler-Baron, V., Sladkevich, I., and Assaraf, Y.G. (2012). Inhibition of the PI3K-Akt signaling pathway disrupts ABCG2-rich extracellular vesicles and overcomes multidrug resistance in breast cancer cells. *Biochem. Pharmacol.* *83*, 1340–1348.
38. Li, W., Zhang, H., Assaraf, Y.G., Zhao, K., Xu, X., Xie, J., Yang, D.H., and Chen, Z.S. (2016). Overcoming ABC transporter-mediated multidrug resistance: molecular mechanisms and novel therapeutic drug strategies. *Drug Resist Updat* *27*, 14–29.
39. Wiese, M., and Stefan, S.M. (2019). The A-B-C of small-molecule ABC transport protein modulators: from inhibition to activation—a case study of multidrug resistance-associated protein 1 (ABCC1). *Med. Res. Rev.* *39*, 2031–2081.
40. Kathawala, R.J., Gupta, P., Ashby, C.R., Jr., and Chen, Z.S. (2015). The modulation of ABC transporter-mediated multidrug resistance in cancer: a review of the past decade. *Drug Resist Updat* *18*, 1–17.
41. Krishna, R., and Mayer, L.D. (2000). Multidrug resistance (MDR) in cancer. Mechanisms, reversal using modulators of MDR and the role of MDR modulators in influencing the pharmacokinetics of anticancer drugs. *Eur. J. Pharm. Sci.* *11*, 265–283.
42. Montesinos, R.N., Moulari, B., Gromand, J., Beduneau, A., Lamprecht, A., and Pelletier, Y. (2014). Coadministration of P-glycoprotein modulators on loperamide pharmacokinetics and brain distribution. *Drug Metab. Dispos* *42*, 700–706.
43. Lopes-Rodrigues, V., Sousa, E., and Vasconcelos, M.H. (2016). Curcumin as a modulator of P-glycoprotein in cancer: challenges and perspectives. *Pharmaceuticals (Basel)* *9*, 71.
44. Hubensack, M., Müller, C., Höcherl, P., Fellner, S., Spruss, T., Bernhardt, G., and Buschauer, A. (2008). Effect of the ABCB1 modulators elacridar and tariquidar on the distribution of paclitaxel in nude mice. *J. Cancer Res. Clin. Oncol.* *134*, 597–607.
45. Wu, S., and Fu, L. (2018). Tyrosine kinase inhibitors enhanced the efficacy of conventional chemotherapeutic agent in multidrug resistant cancer cells. *Mol. Cancer* *17*, 25.
46. Hegedus, T., Orfi, L., Seprodi, A., Váradi, A., Sarkadi, B., and Kéri, G. (2002). Interaction of tyrosine kinase inhibitors with the human multidrug transporter proteins, MDR1 and MRP1. *Biochim. Biophys. Acta* *1587*, 318–325.
47. Shi, Z., Liang, Y.J., Chen, Z.S., Wang, X.W., Wang, X.H., Ding, Y., Chen, L.M., Yang, X.P., and Fu, L.W. (2006). Reversal of MDR1/P-glycoprotein-mediated multidrug resistance by vector-based RNA interference in vitro and in vivo. *Cancer Biol. Ther.* *5*, 39–47.
48. Xiang, Q.F., Zhang, D.M., Wang, J.N., Zhang, H.W., Zheng, Z.Y., Yu, D.C., Li, Y.J., Xu, J., Chen, Y.J., and Shang, C.Z. (2015). Cabozantinib reverses multidrug resistance of human hepatoma HepG2/adr cells by modulating the function of P-glycoprotein. *Liver Int.* *35*, 1010–1023.
49. Li, K., Zhang, H., Qiu, J., Lin, Y., Liang, J., Xiao, X., Fu, L., Wang, F., Cai, J., Tan, Y., et al. (2016). Activation of cyclic adenosine monophosphate pathway increases the sensitivity of cancer cells to the oncolytic virus M1. *Mol. Ther.* *24*, 156–165.
50. Fu, L., Liang, Y., Deng, L., Ding, Y., Chen, L., Ye, Y., Yang, X., and Pan, Q. (2004). Characterization of tetrandrine, a potent inhibitor of P-glycoprotein-mediated multidrug resistance. *Cancer Chemother. Pharmacol.* *53*, 349–356.
51. Ford, J.M., and Hait, W.N. (1990). Pharmacology of drugs that alter multidrug resistance in cancer. *Pharmacol. Rev.* *42*, 155–199.
52. Zhou, W.J., Zhang, X., Cheng, C., Wang, F., Wang, X.K., Liang, Y.J., To, K.K., Zhou, W., Huang, H.B., and Fu, L.W. (2012). Crizotinib (PF-02341066) reverses multidrug resistance in cancer cells by inhibiting the function of P-glycoprotein. *Br. J. Pharmacol.* *166*, 1669–1683.
53. Ambudkar, S.V. (1998). Drug-stimulatable ATPase activity in crude membranes of human MDR1-transfected mammalian cells. *Methods Enzymol.* *292*, 504–514.
54. Dai, C.L., Tiwari, A.K., Wu, C.P., Su, X.D., Wang, S.R., Liu, D.G., Ashby, C.R., Jr., Huang, Y., Robey, R.W., Liang, Y.J., et al. (2008). Lapatinib (Tykerb, GW572016) reverses multidrug resistance in cancer cells by inhibiting the activity of ATP-binding cassette subfamily B member 1 and G member 2. *Cancer Res.* *68*, 7905–7914.